# Environment of the Early Pleistocene Banshan Paleolithic Site in the Nihewan Basin, North China

Jiaxing Yang[1,2,3], Zhen Zhang[1,2,3]*, Yuecong Li[1,2,3]*, Fagang Wang[4], Baoshuo Fan[1,2,3], Zijing She[1,2,3], Hongli Xie[1,2,3], Siyu Wang[1,2,3] and Shuoqiang Da[1,2,3]

[1]College of Geographical Sciences, Hebei Normal University, Shijiazhuang, China, [2]Hebei Key Laboratory of Environmental Change and Ecological Construction, Shijiazhuang, China, [3]Hebei Technology Innovation Center for Remote Sensing Identification of Environmental Change, Shijiazhuang, China, [4]Hebei Provincial Institute of Cultural Relics and Archaeology, Shijiazhuang, China

The Banshan archaeological site is one of the most important Early Pleistocene Paleolithic sites in the Nihewan Basin in North China. Based on analyses of pollen, grain size and charcoal of 56 samples from a sedimentary profile, we reconstructed the environment of the Banshan site before and after the interval of hominin activity (1.340–1.290 Ma). The results show that before the appearance of hominin activity (1.340–1.324 Ma), the climate of the region was initially cold and wet and then cold and dry. The regional vegetation was mainly *Pinus* and *Picea* forest in the earlier stage, and steppe dominated by arid-tolerant plants such as *Artemisia* and Chenopodiaceae in the later stage. During the period of hominin activity (1.324–1.318 Ma), the climate was warm and wet, the vegetation was mainly *Pinus* forest, and the site was a lakeside environment which would have provided resources such as food and water for hominins. During 1.318–1.310 Ma, the climate was warm and wet, the lake continued to expand and the lake level rose, which may have forced the hominins to migrate outside the area. During 1.310–1.290 Ma, the climate changed from warm and humid to cold and arid, accompanied by the change of the regional vegetation from forest to forest-grassland. Hominin activity at the Banshan site occurred during the interval of climate change from cold and dry to warm and wet, and it ended with the rise of the ancient lake level at Nihewan and the deterioration of the climate.

Keywords: Nihewan Basin, Banshan site, Environmental context, Palaeovegetation, Palaeoclimate
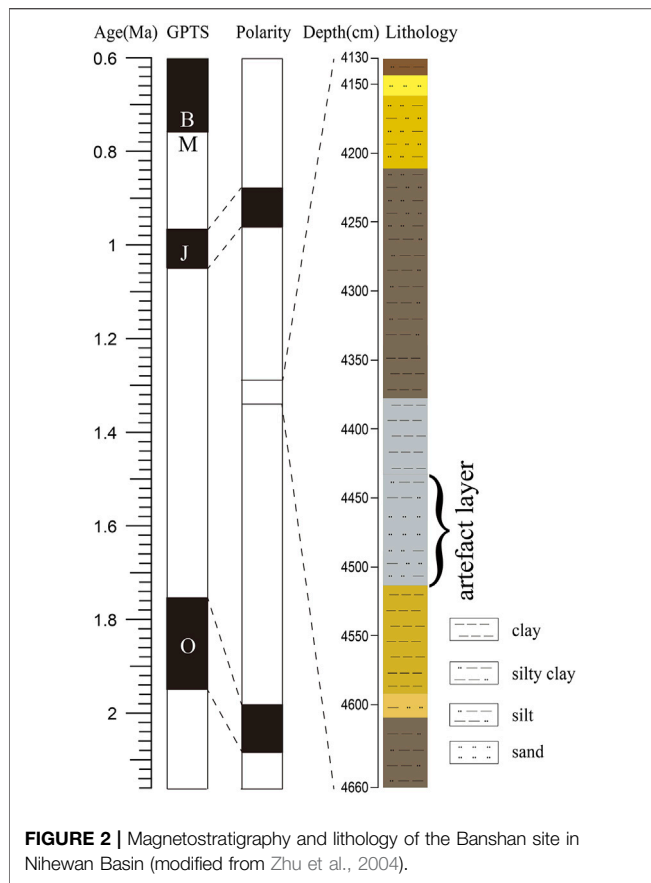
## INTRODUCTION

The Early Pleistocene was an important period of global climate change (Leinen and Health, 1981; Bailey et al., 2012), and also an important stage in the emergence and evolution of hominins (Bonnefille, 2010; Colcord et al., 2018). Hence, there is much research interest in determining the climatic and environmental context of Early Pleistocene hominin sites in order to explore the relationship between climate change and human evolution. The Nihewan Basin in North China has both the largest number and highest concentration of earliest Pleistocene archaeological sites in East Asia (Xie, 2006; Yuan et al., 2011), and the Nihewan Basin is also the northernmost documented location of early human activities in East Asia (Zhu et al., 2004; Deng et al., 2008; Dennell, 2013). It is also a key area for studying the relationship between environment and early human evolution in East Asia, especially in North China (Barbour, 1924; Chen, 1988; Zhou et al., 1991; Yuan et al., 2011; Ao et al., 2017; Deng et al., 2019; Yang et al., 2020), with a long history of research activity. Since the

FIGURE 1 | Location of the Nihewan Basin in China **(A)**. The topography of the study area together with the location of the sampling site **(B)** and the field photograph of sampling site **(C)**. (Altitudes are in m a.s.l.).
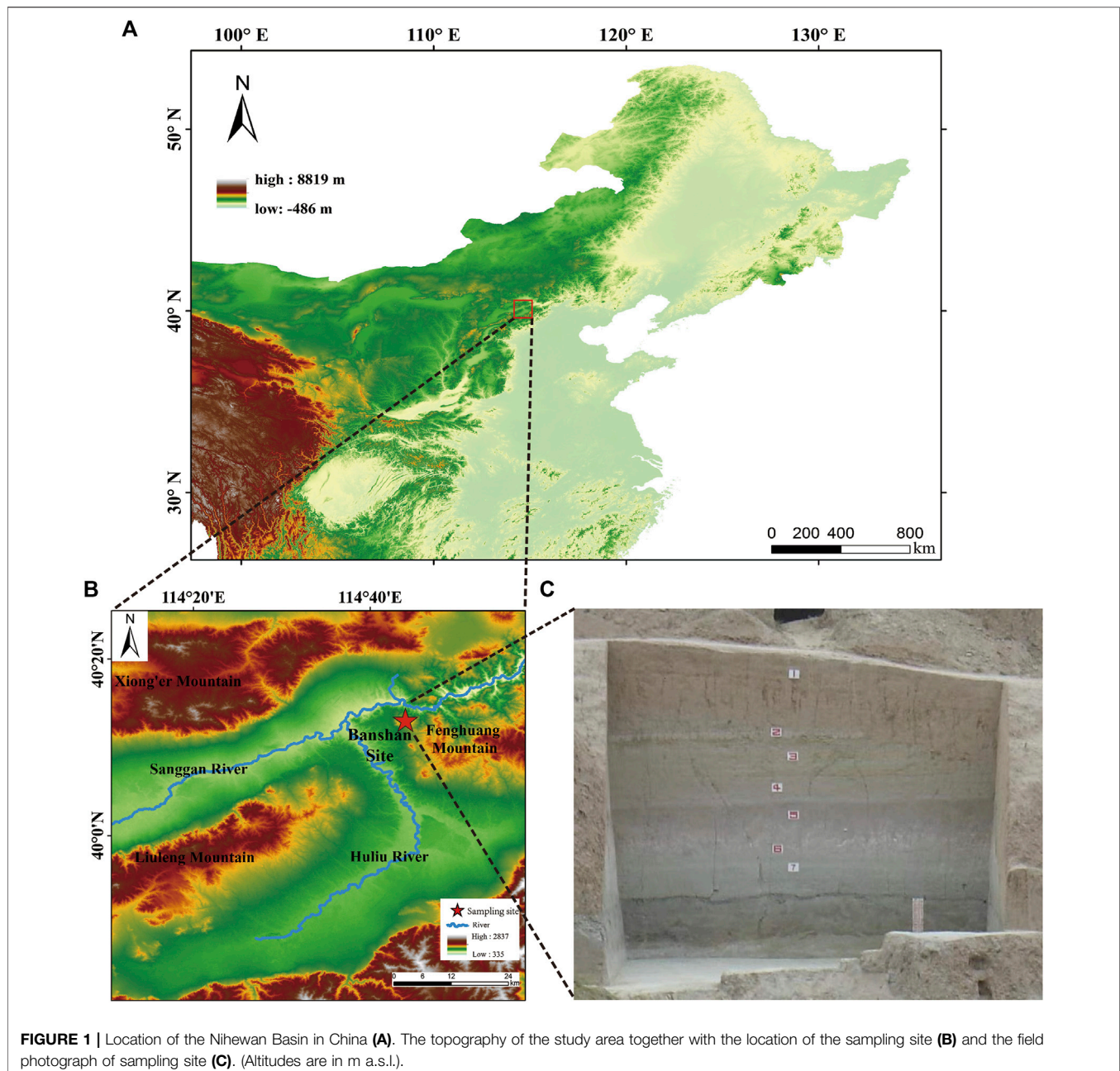
1920s, studies of the archaeology, paleoanthropology, chronology, and climate record of the Nihewan Basin have provided much valuable results (Zhu et al., 2001; Zhu et al., 2004; Ao et al., 2013a; Li et al., 2019; Ding et al., 2020; Zhang et al., 2020; Zhang et al., 2021), especially based on the excavation of Early Pleistocene sites combined with accurate dating (Wang et al., 2004; Zhu et al., 2004; Deng et al., 2008; Liu et al., 2011; Ao et al., 2013b; Liu et al., 2018). The results have enabled a relatively complete cultural sequence of Early Pleistocene paleo-human evolution in the Nihewan Basin to be established (Xie et al., 2004; Zuo et al., 2011; Liu et al., 2013; Pei et al., 2017; Deng et al., 2019; Yang et al., 2020). From these studies it has emerged that the Early Pleistocene (1.4–1.1 Ma) in the Nihewan Basin was characterized

by a relatively high level of hominin activity. Several archaeological sites are dated to this interval, including Xiaochangliang (1.36 Ma) (Xia and Liu, 1984; Tang et al., 1995; Chen et al., 1999; Yang et al., 2016), Dachangliang (1.36 Ma) (Pei, 2002; Deng et al., 2006), Banshan (1.32 Ma) (Wei, 1994; Zhu et al., 2004), Feiliang (1.2 Ma) (Li et al., 1996; Ao et al., 2012a; Pei et al., 2017), Donggutuo (1.1 Ma) (Pei et al., 2009; Wei, 2014) and CenJiawan (1.1 Ma) (Xie and Cheng, 1990; Wang et al., 2006; Guan et al., 2016). However, there is a lack of studies of the environmental context of hominin activities during this period; moreover, some of the conclusions of the previous environmental reconstructions for these sites are contradictory. For example, pollen studies have indicated that the vegetation at

FIGURE 2 | Magnetostratigraphy and lithology of the Banshan site in Nihewan Basin (modified from Zhu et al., 2004).

Dachangliang (1.36 Ma) and Feiliang (1.2 Ma) was mainly grassland; whereas the environment of the Donggutuo site (1.1 Ma) was forest and grassland (Pei et al., 2009). Moreover, there are differences in the environmental characteristics revealed by the application of different proxies at the same site. For example, a study of mammal fossils at Xiaochangliang (1.36 Ma) revealed the presence of *Coelodonta antiquitatis*, *Palaeoloxodon* sp. and *Viverra,* which are characteristic of forest habitats, as well as *Bison*, *Equus samenensis* and *Hipparion,* which are grassland animals (Tang et al., 1995). In the Xiaochangliang area, tree pollen was found to be dominant in the late Early Pleistocene, indicating mainly forest vegetation (Xia and Liu, 1984). Low temporal resolution is one of the main reasons for these difference. Therefore, more studies with a higher temporal resolution are needed to determine the Early Pleistocene environment of early humans in the Nihewan Basin.

Banshan is an important early Paleolithic site in the Nihewan Basin (Wei, 1994). The site was first excavated in the early 1990s, and a large area to the southeast of the original excavation was excavated in 2003 (Xie, 2006). Paleomagnetic dating results showed that age of the artefact layer at the site is 1.32 Ma (Zhu et al., 2004). In addition to stone cores, a large number of lithic fragments and scrapers were discovered (Wei, 1994; Xie, 2006). Although no evidence of surface repair technology was found, unlike the case of the lithic tools unearthed at the Donggutuo site (Wei, 2014), which were produced by

hammering, significant progress had been made in materials selection and processing methods compared with older sites. Additionally, several stone tools had wide and deep repair scars (Xie, 2006). The lithic processing technology at Banshan makes it an important site for studying the migration, diffusion and technological exchange of ancient humans in Northeast Asia during the Early Pleistocene (Hou, 2003). However, while the chronology and archaeology of the Banshan site are well established, the environmental background of the site is relatively poorly documented.

Here, we present the results of a study of pollen and spores, grain size and charcoal particles from a profile at Banshan. Our aims were to determine in detail the pattern of environmental change, especially the climate and vegetation, during the interval of hominin activity (1.34–1.29 Ma), and hence to better understand Early Pleistocene hominin evolution and expansion in the Nihewan Basin and its driving mechanisms.

## SETTING, SAMPLES AND CHRONOLOGY

### Geology

The Nihewan Basin (40°05′–40°20′N, 114°25′–114°44′E) (Figure 1) is located in Yangyuan County, Hebei Province, China. The area of the basin is ~ 2,000 km$^2$ and the average elevation is ~ 1,000 m. The basin is surrounded by the Xiong'er Mountains to the north, the Liuleng Mountains to the south, and the Fenghuang Mountains to the east. The Nihewan paleo-lake basin began to develop in the Middle-Late Pliocene (Ao et al., 2013c; Liu et al., 2018) and was infilled with a thick layer of Plio-Pleistocene fluvio-lacustrine strata. The elevation of the block and the resulting intensification of erosion caused the draining of the lake, and the deposition of late Middle Pleistocene lacustrine strata ceased (Zhou et al., 1991; Deng et al., 2019).

### Stratigraphy of the Banshan Profile and Sampling

The Banshan site is located in the eastern part of the Nihewan Basin (40°13 '31 "N, 114°39′ 50″E) (Figure 1). In 1990, Wei Qi and Cheng Shengquan, of the Institute of Vertebrate Paleontology and Paleoanthropology of the Chinese Academy of Sciences, conducted a trial excavation and made detailed observations at the site (Wei, 1994). In 2003, the Institute of Cultural Relics of Hebei Province excavated a site to the southeast of the original excavation area, and discovered over 1,600 relics such as lithic tools, together with animal remains, within the artefact layer, indicating that ancient humans used the artefacts for dismembering animals (Xie, 2006).

The section is located on the third terrace of the Sanggan River, within fluvial-lacustrine strata at the top of the MJG-I artefact layer of the Majuangou site (Xie, 2006). The formation is mainly composed of grayish-brown silty sand and grayish-brown silty clay, with occasional fine gravel, and comprises lacustrine lakeshore facies. The section is stratigraphically continuous and there are no obvious sedimentary discontinuities. In 2016, environmental archaeology samples were collected by the College

of Resources and Environmental Science of Hebei Normal University. The depth of the artefact layer was 45.1–44.3 m, the total thickness of the profile was 5.45 m, and the depth range was 41.15–46.60 m. Samples were collected at 10-cm intervals, yielding a total of 56 samples.

## METHODS

### Chronology

A detailed magnetostratigraphy provides precise age controls for the Banshan section, and the depth interval of 41.3–46.6 m has an estimated age range of 1.29–1.34 Ma (Zhu et al., 2004). The ages of the 56 pollen samples used in the present study were estimated by linear interpolation between geomagnetic polarity reversal boundaries and by extrapolation of the average sediment accumulation rate. Accordingly, the samples, which are from the depth interval of 41.3–46.6 m, have an age range of 1.29–1.34 Ma. This approach was deemed appropriate because the sediment accumulation rate appears to be relatively continuous within each interval (**Figure 2**).

The paleomagnetic age of the depth of the artefact layer (44.7 m) in the Banshan section is 1.32 Ma, and that of the depth of the MJG-I artefact layer (65.3 m) (Zhu et al., 2004), which is connected to the Banshan section, has the paleomagnetic age of 1.55 Ma. The average sediment accumulation rate of the studied interval is therefore estimated to be 11.17 kyr/m, and based on interpolation the age of the section is ~ 1.34–1.29 Ma.

### Pollen and Spore Extraction and Identification

Pollen and spores were concentrated using a modified HCL-NaOH-HF procedure (Faegri and Iversen, 1989). For each sample, 300 g of sediment was weighed before chemical treatment and one tablet of *Lycopodium* spores (27,560 grains/tablet) was added to calculate the pollen concentration. After chemical treatment, pollen and spores were extracted using heavy liquid (1.98 g/cm$^3$) flotation. The procedures were carried out at the College of Resources and Environmental Sciences of Hebei Normal University. Pollen and spores were identified and counted using a Zeiss Imager A2 optical microscope at × 400 magnification. For most samples, more than 400 identified pollen and spores were counted. The morphological identification was carried out with reference to Wang et al. (1995) and Tang et al. (2016).

### Principal Component Analysis

Principal component analysis (PCA) is widely used in ecology and related fields (Davies and Fall, 2001), and is useful for simplifying complex multivariate datasets (Zhang et al., 2013; Li et al., 2018). To better understand the environmental implications of the major pollen types at the Banshan site, eight pollen types (*Pinus, Picea + Abies, Betula,* Elaeagnaceae, *Artemisia,* Chenopodiaceae, Poaceae, and *Urtica + Humulus*), each with an average representation >1% (86.5% of the total pollen). In order to reduce the error, the square-root transformed

pollen data were used for PCA which was implemented with Canoco 5 software (Braak and Smilauer, 2012).

### Grain-Size Analysis

Grain-size analysis was used to characterize the sedimentary environment. Fifty-six samples were pre-treated using conventional methods to remove organic matter and calcium carbonate. Grain-size distributions were measured with a Mastersizer 3,000 laser diffraction analyzer (Malvern Instruments, UK) with a measurement range of 0.01–3,500 μm. Measurements were performed at shading rates of 15–20% and were repeated three times, with a systematic error of <3% (Peng et al., 2005). Based on the Udden-Wentworth scale, sediments were divided into clay (<4 μm), silt (4–63 μm) and sand (>63 μm) according to the particle size (Friedman and Sanders, 1978). Grain-size frequency distributions and cumulative curves were plotted to determine the sedimentary environment. The grain-size frequency distribution curves directly reflect the grain-size distribution characteristics of sediments, and the cumulative curves can be divided into stage corresponding to the transport mode of sedimentary particles by creep, saltation, and in suspension, providing information about the dynamics of the sedimentary environment. Based on the grain-size cumulative curves distributions characteristics, the intervals of creep, saltation, and suspension are < 2φ (>256 μm), 2-5φ(256–32 μm) and > 5φ(<32 μm), respectively. (Jiang, 2010; Yuan et al., 2013).

### Charcoal Analysis

Charcoals are dark brown or black porous inorganic carbon compounds produced by the incomplete combustion or pyrolysis of organisms. It is often used to indicate the occurrence of fire and the abundance of biomass in paleoclimate studies (Miao et al., 2016; Shi et al., 2020). Charcoal was extracted using a modified pollen procedure (HCL-NaOH-HF) (Faegri and Iversen, 1989), and identified and counted using a Zeiss Imager A2 optical microscope at ×400 magnification. Based on the length of the principal axis, the numbers of particles of coarse (>125 μm), medium (450–125 μm) and fine (<50 μm) were counted (Miao et al., 2016). Lycopodium spores (27,560 grains/tablet) in the samples were counted to calculate the charcoal concentration. More than 1,000 charcoal particles were counted for each sample.

## RESULTS

### Pollen Assemblages in the Early Pleistocene Interval (1.34–1.29 Ma) of the Banshan Site

Sixty pollen and spore types were identified within the 56 pollen samples from the Banshan profile, including 15 arboreal taxa, 10 shrub taxa, 30 herb taxa, and 5 fern spore taxa. A total of 37,668 pollen and spores were counted (excluding algae), and an average of 673 pollen and spores for each sample, with an average concentration of 96 grains/g. Among the identified taxa, *Pinus,*
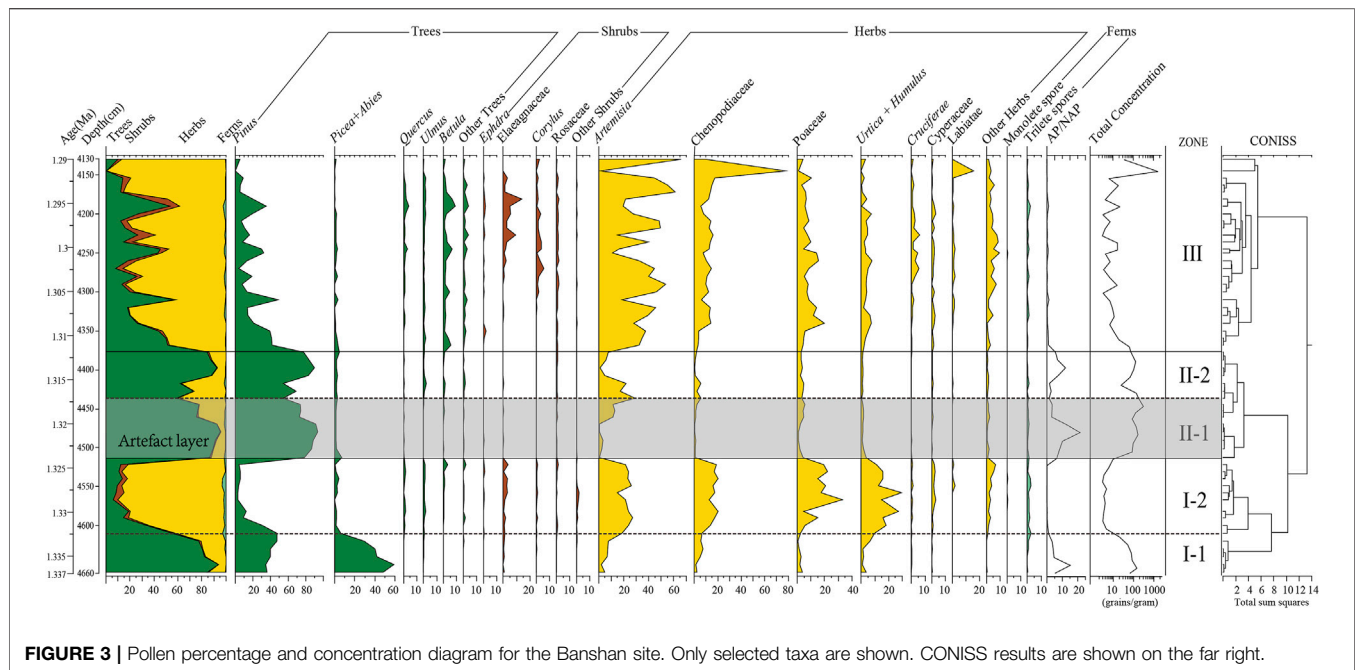
**FIGURE 3 |** Pollen percentage and concentration diagram for the Banshan site. Only selected taxa are shown. CONISS results are shown on the far right.

*Picea*, *Abies*, *Quercus*, *Ulmus* and *Betula* are the most common arboreal pollen types; *Elaeagnus*, *Corylus* and Rosaceae are the most common shrub pollen types; *Artemisia*, Chenopodiaceae, Poaceae, Brassicaceae, Labiatae, Cyperaceae, *Urtica* and *Humulus* are the most common herb pollen types; and *Selaginella* is the dominant fern spore type. The pollen record reveals alternations of the dominance of tree pollen and herb pollen, with respective maximum and average representations of 95.6 and 45.8% for trees, and 99.5 and 48.8% for herbs. The average shrub pollen content is 3.1%, while the fern spore content is very low, with an average of 0.7%. According to CONISS clustering analysis results, the pollen record can be divided into three pollen assemblages zones (**Figure 3**), which are described below.

Zone I (46.60–45.13 m; 1.337–1.324 Ma; 15 samples). The pollen assemblage is dominated by *Picea* or *Artemisia* alternately, which can be divided into two sub-zones according to different pollen assemblages.

Zone I-1 (46.6–46.1 m; 1.337–1.333 Ma; 5 samples). The average pollen count is 720 and the average pollen concentration is 102 grains/g. Tree pollen is dominant, with an average of 79% (range: 55.3–93.8%). *Pinus* (average: 40.9%) and *Picea + Abies* (average: 37.5%) are the main tree pollen types. The average representation of broadleaved trees is <1%. The average shrub pollen representation is 1.1%, comprising Elaeagnaceae, Rosaceae and *Corylus*. The average herb pollen representation is 19.1% (range: 6.2–38.9%); *Artemisia* and Chenopodiaceae vary between 1 and 6%; Poaceae, *Urtica + Humulus* are less common (<2%), and Cyperaceae and Labiatae are rare.
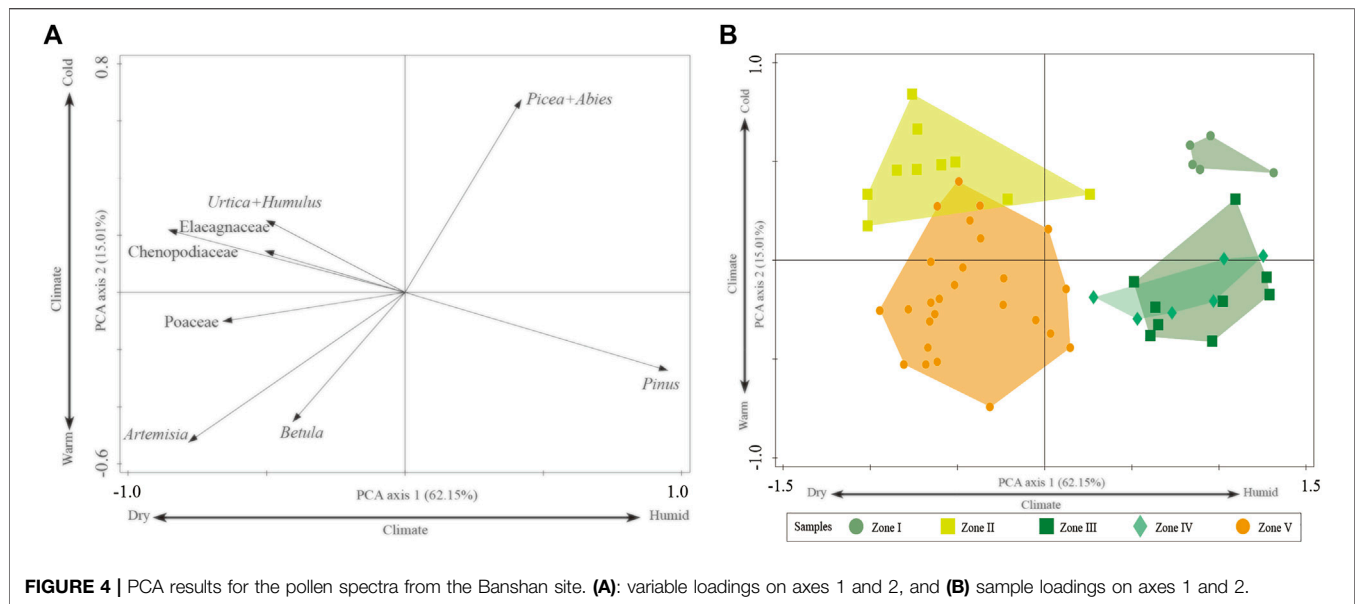
Zone I-2 (46.10–45.13 m; 1.333–1.324 Ma; 10 samples). The average pollen count is 433, and the average pollen concentration is 6 grains/g, which is the lowest within the studied interval. Herb pollen is dominant, with an average of 80.3% (range: 63.2–88.2%), and has the highest representation within the studied interval.

*Artemisia,* Chenopodiaceae, Poaceae, and *Urtica + Humulus* have a roughly uniform representation ( ~ 20%). The average shrub pollen representation is 3.9% (range: 1.6–6.8%), which is slightly higher than zone I; Elaeagnaceae is the dominant taxon (average: 1.8%). The tree pollen representation is substantially lower than in Zone I-1, with an average of 14.3% (range: 6.4–33.8%), and is the lowest within the studied interval. In particular, there are substantial decreases in *Pinus* (average: 8.8%) and *Picea + Abies* (average: 1.9%).

Zone II (45.13–43.77 m; 1.324–1.312 Ma; 15 samples). The average pollen count is 807 and the average pollen concentration is 157 grains/g. Arboreal pollen is dominant, with an average of 82.1% (range: 59.1–95.6%). *Pinus,* with an average of 78.2% (range: 54.4–93.7%) is the main arboreal pollen types. Compared with Zone I-2, the herb pollen representation is substantially lower and is the lowest within the studied interval, with an average of 16.6% (range: 3.8–39.1%). *Artemisia* (average: 8.1%) and Poaceae (average: 3.2%) are the most common herb pollen types.

The artefact layer located in this Zone (45.13–44.36 m; 1.324–1.317 Ma; 9 samples). The pollen assemblage is similar with the Zone II, while the average pollen concentration is 182 grains/g, which is the highest within the studied interval.

Zone III (43.77–41.30 m; 1.312–1.290 Ma; 26 samples). The average pollen count is 667 pollen and the average pollen concentration is 121 grains/g, which is less than in Zone II. Herb pollen is dominant, with an average of 68.3% (range: 35.9–99.6%); the main taxa are *Artemisia* (average: 35.6%), followed by Chenopodiaceae (average: 13.4%) and Poaceae (average: 7.9%). The average tree pollen representation is 25.9% (range: 0.3–57.2%), which is substantially lower than in Zone II. The average *Pinus* representation is 18.6% (range: 0.2–48.8%), and *Picea + Abies* are present at a low level (average: 1.1%). The representation of broadleaved trees

**FIGURE 4** | PCA results for the pollen spectra from the Banshan site. **(A)**: variable loadings on axes 1 and 2, and **(B)** sample loadings on axes 1 and 2.

(minimum of 4%, average of 6.2%, and range of 0.1–17.9%) is higher than in the previous zone, but with a decreasing trend through the zone.

## Principal Component Analysis

The first principal component explains 62.15% of the total variance and the first and second principal components together explain 77.16%; hence, the first two components provide a parsimonious summary of the pollen data. Biplots of the variable and sample loadings on axes 1 and 2 are illustrated in **Figure 4**. Tree taxa preferring relatively wet conditions (*Pinus* and *Picea + Abies*) have positive loadings on axis 1, and drought tolerant taxa (*Artemisia*, Chenopodiaceae, Poaceae and Elaeagnaceae) have negative loadings on axis 1; hence, axis 1 can be interpreted to reflect changes between wetter and drier conditions. Cold-tolerant taxa (*Picea + Abies* and Elaeagnaceae) have positive loadings on axis 2, and the warm-preference *Pinus* has negative loadings on axis 2; hence, this axis may reflect a gradient in temperature conditions. On this basis the four quadrants of the coordinate system from the first to the fourth can be classified as follows: cold-wet, cold-dry, warm-dry and warm-wet, respectively.

Reference to **Figure 4** shows that samples of Zone I are distributed in the first quadrant, indicating that the climate at this time was mainly cold and wet. The samples of Zone II are concentrated in the second quadrant, indicating that the climate was mainly cold and dry. The samples from Zone III and Zone IV are mainly distributed in the fourth quadrant, indicating that the climate during these intervals was warm and humid. The samples in Zone V are concentrated in the third quadrant, indicating that the climate was mainly warm and dry.
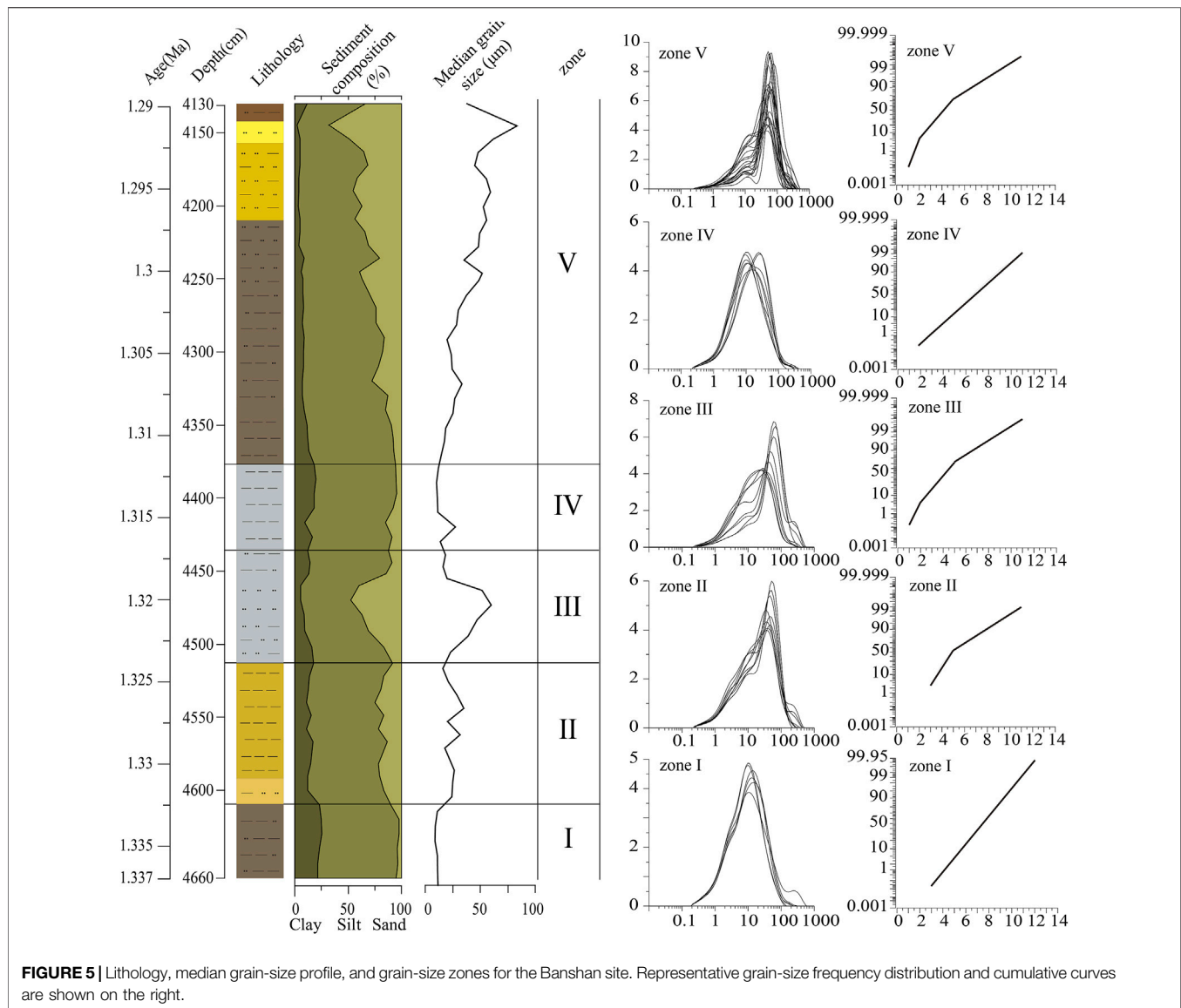
## Grain-Size Distribution

The percentage of clay (<4 μm) in the samples ranges from 2.1 to 25.6% (average: 11.7%); the percentage of silt (4–63 μm) ranges

from 29.9 to 80.0% (average: 66.4%); the percentage of sand (>63 μm) ranges from 2.3 to 68.0% (average: 21.9%); and the median grain size (Md) ranges from 8.9 to 83.5 μm (average: 30.4 μm). Thus, the sediments within the profile are relatively fine-grained. Most of the grain-size frequency distribution curves are unimodal, but a few samples are multi-modal with small secondary peaks or a double peak. The cumulative curves show that most samples are mainly saltation and suspension components, with a few samples also containing a creep component. The slope gradients are shallow, indicating that the samples are poorly sorted and are derived from a local source. Based on the grain-size distributions characteristics the profile can be divided into five intervals, which correspond to the pollen assemblage zones (**Figure 5**), and they are described below.

Zone I (46.6–46.1 m; 1.337–1.333 Ma) is mainly grayish-brown silty clay. The sediments are fine-grained (median grain size 10.4 μm, range: 8.9–11.6 μm). The average clay content is 23.4% (range: 21.4–25.6%), which is the highest in the section; the average silt content is 73.1% (range: 72.1–74.7%), and the average sand content is 3.4% (range: 2.3–5.1%), which is the lowest in the studied interval. The grain-size frequency distribution curves are unimodal, and the cumulative curves generally lack a creep component; the saltation component is very low (<3%) and the suspension component is dominant.

Zone II (46.10–45.13 m; 1.333–1.324 Ma) is mainly yellowish-brown clay. The median grain size is larger than in Zone I, with an average of 24.1 μm (range: 11.0–35.1 μm). The average clay content is 14.5% (range: 11.2–23.1%), and the average silt content is 67.4% (range: 63.6–70.9%), which are lower than in Zone I. The average sand content is 18.2% (range: 10.3–24.8%), which is higher than in Zone I. The grain-size frequency distribution curves are mainly unimodal, and the cumulative curve consists of two stages; a creep component is lacking, the saltation component is just above 50%, and the suspended component is <50%.

**FIGURE 5 |** Lithology, median grain-size profile, and grain-size zones for the Banshan site. Representative grain-size frequency distribution and cumulative curves are shown on the right.

Zone III (45.13–44.36 m; 1.324–1.317 Ma). This zone corresponds to the artefact layer. It is mainly gray and grayish-brown clay silt. The grain size is coarse (median 32.4 μm, range: 16–60 μm). The average clay content is 11.5% (range: 5.7–17.7%), and the average silt content is 64.4% (range: 46.7–76.4%), which are lower than that in Zone II. The average sand content is 24.1% (range: 8.7–47.5%), which is higher than in Zone II. The grain-size frequency distribution curves are mainly unimodal, and the cumulative curves indicate three stages. The creep component is only 5%, the saltation component content is nearly 70%, and the suspended component content is 25%.

Zone IV (44.36–3.77 m; 1.317–1.312 Ma) is mainly light-gray clay. The sediments are fine grained (median 14.3 μm, range: 10.3–27.4 μm). The average clay content is 16.9% (range: 9.4–20.2%); the average silt content is 75.3% (range: 73.9–77.2%), which is the highest in the studied interval; and the average sand content is 7.8% (range: 4.4–15.0%), which is the

lowest. The grain-size frequency distribution curves are unimodal, and the cumulative curve indicates a single stage, lacking a creep component. Several samples lack a saltation component, and the saltation component is mainly <10%, and the suspended component is ~ 90%.

Zone V (43.68–41.30 m; 1.312–1.290 Ma) is mainly grayish-brown and brownish-yellow silt. The median grain size is 10.4 μm (range: 8.9–11.6 μm). The average clay content is 7.3% (range: 2.1–13.4%), which is the lowest in the studied interval; the average silt content is 63.3% (range: 29.9–80.0%), which is lower than in Zone IV; and the average sand content is 29.4% (range: 7.5–68.0%), which is the highest in the studied interval. The grain-size frequency distribution curves are mainly unimodal, but several samples have smaller sub-peaks or are bimodal. The cumulative curve shows three well-defined stages, with a creep component of only 5%, a saltation component of nearly 70%, and a suspension component of 25%.
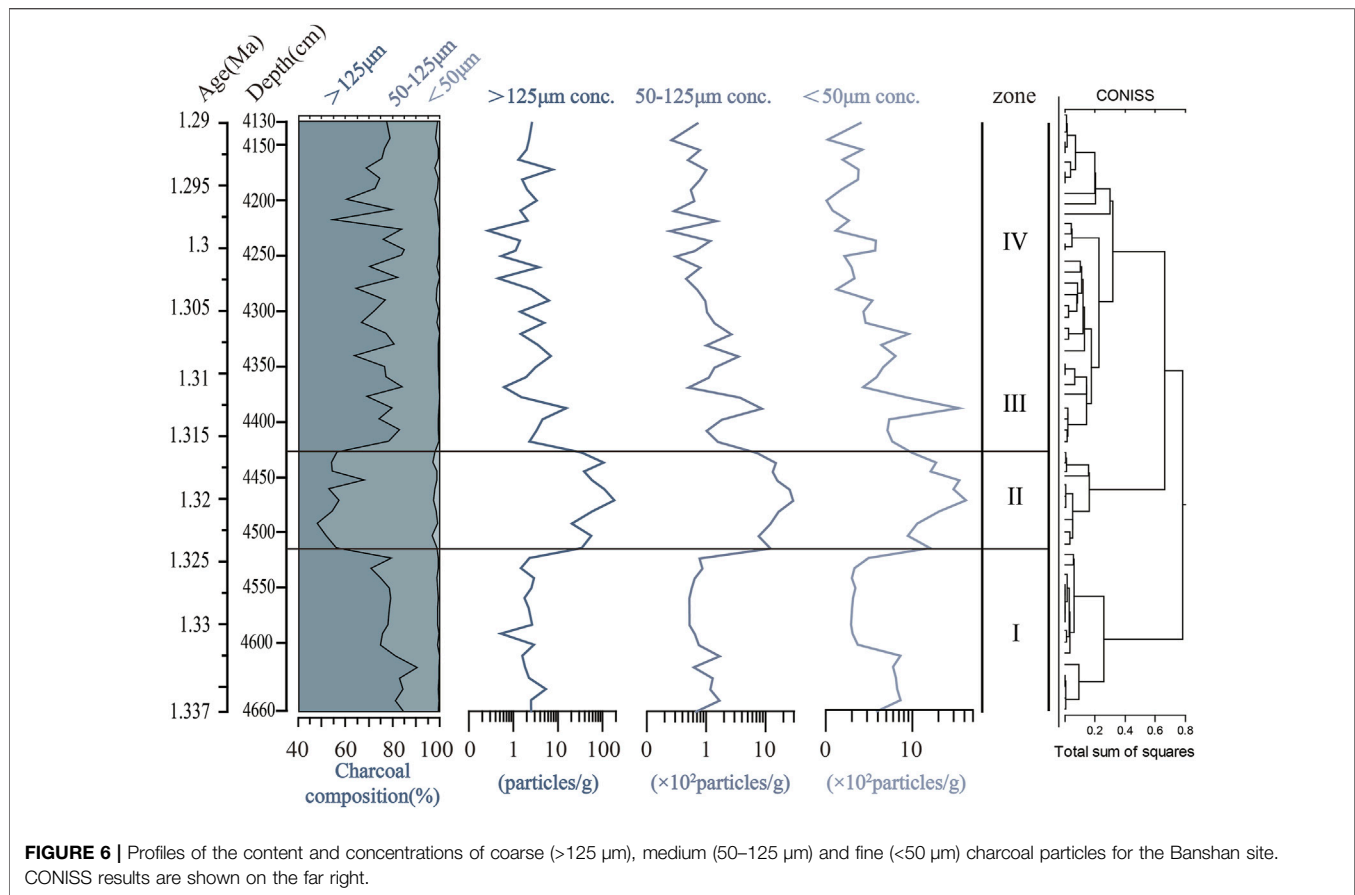
**FIGURE 6** | Profiles of the content and concentrations of coarse (>125 μm), medium (50–125 μm) and fine (<50 μm) charcoal particles for the Banshan site. CONISS results are shown on the far right.

## Charcoal Distribution

The results of the charcoal analysis are shown in **Figure 6**. The average charcoal concentration of the 56 samples is 1,099 particles/g; the particles are mainly fine, with an average content of 72.8% and an average concentration of 712 particles/g. The average content of medium charcoal particles is 26.3%, with the average concentration of 372 particles/g; and the average content of coarse particles is only 0.9%, with an average concentration of 15 particles/g. Combined with the results of CONISS analysis, the charcoal profiles are divided into three zones, which are described below (**Figure 6**).

Zone I (46.60–45.13 m; 1.337–1.324 Ma) has a low average charcoal concentration of 472 particles/g, with average concentrations of fine, medium and coarse particles of 383 particles/g, 86 particles/g and 2 particles/g, respectively. The content of fine, medium and coarse particles are 79.75, 19.65 and 0.60%, respectively.
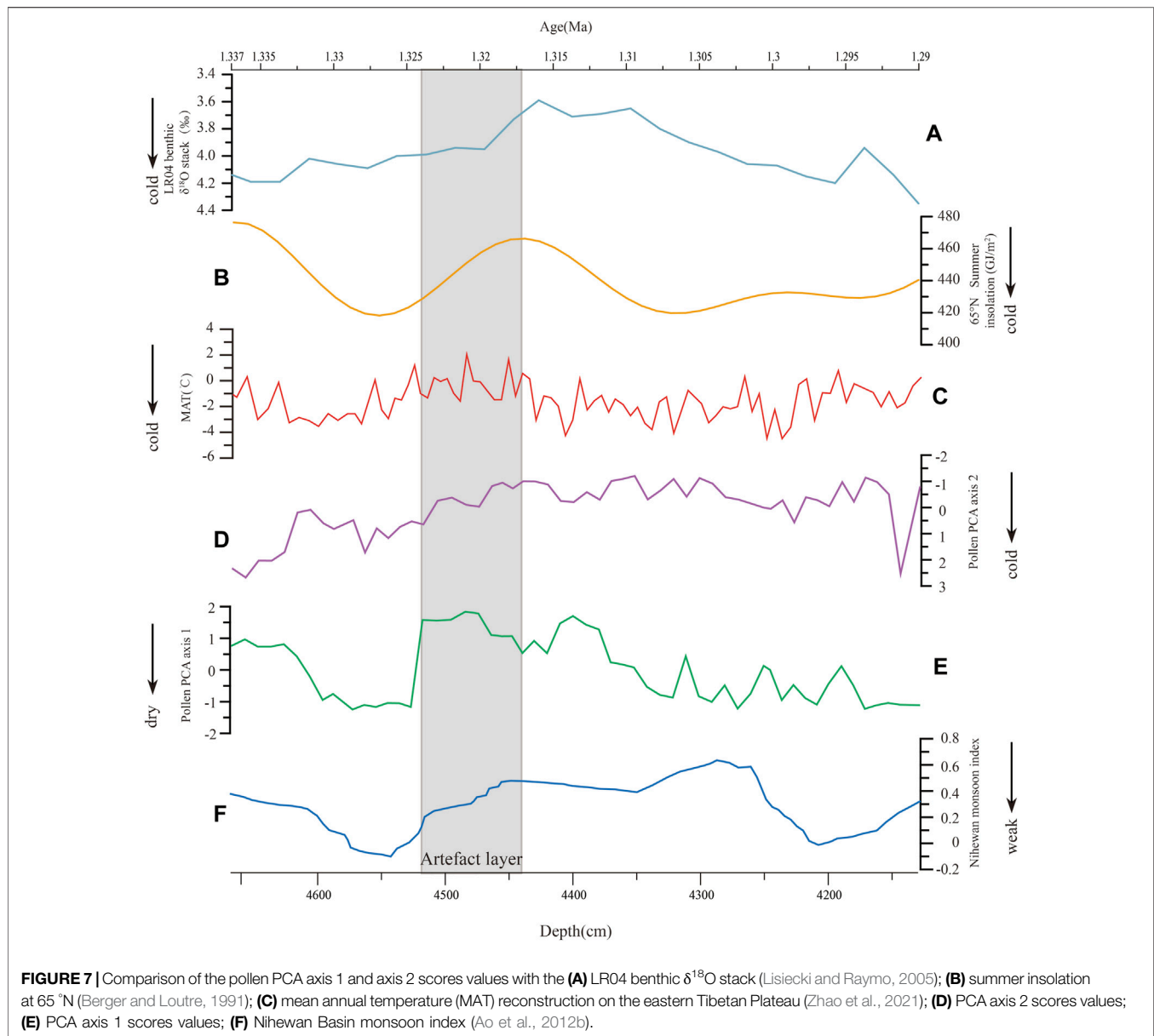
Zone II (45.13–44.36 m; 1.324–1.317 Ma) corresponds to the artefact layer. The average charcoal concentration is the highest in the section, with an average of 3,906 particles/g, with average concentrations of fine, medium and coarse particles of 2,200 particles/g, 1,631 particles/g, and 74 particles/g, respectively. The average content of fine particle (55.28%) is the lowest in all the profile; on the contrary, the average content of medium and coarse particles are 42.85 and 1.87%, which are the highest in all the profile.

Zone III (44.36–43.77 m; 1.317–1.290 Ma). The average charcoal concentration is 604 particles/g, and the range is greater than in the other zones (134–4333 particles/g). The average concentrations of fine, medium and coarse charcoal particles are 447 particles/g, 153 particles/g, and 4 particles/g, respectively. The average content of fine, medium and coarse particles are 74.49, 24.76 and 0.75%, respectively.

## DISCUSSION

### Environmental Characteristics of the Banshan Site Before the Appearance of Hominins (1.337–1.324 Ma)

During the interval before the appearance of hominin activity at the Banshan site, the pollen assemblage was dominated by cold-tolerant *Picea* (Zhao et al., 2009; Lu et al., 2011) and drought-tolerant *Artemisia* and Chenopodiaceae (Sun et al., 1996; Xu et al., 2017), indicating that the vegetation was coniferous forest dominated by *Picea,* or steppe dominated by *Artemisia* and Chenopodiaceae. The overall climate was cold, but there were fluctuations between drier and wetter conditions. During 1.337–1.333 Ma, *Pinus* and *Picea* dominated the pollen assemblage. Indicating that the local vegetation was coniferous forest dominated by *Picea* and *Pinus*, possibly with *Picea*

**FIGURE 7 |** Comparison of the pollen PCA axis 1 and axis 2 scores values with the **(A)** LR04 benthic δ¹⁸O stack (Lisiecki and Raymo, 2005); **(B)** summer insolation at 65 °N (Berger and Loutre, 1991); **(C)** mean annual temperature (MAT) reconstruction on the eastern Tibetan Plateau (Zhao et al., 2021); **(D)** PCA axis 2 scores values; **(E)** PCA axis 1 scores values; **(F)** Nihewan Basin monsoon index (Ao et al., 2012b).

dominant at higher elevations; *Pinus* was more likely to occur at lower elevations. The cold and wet climate was not conducive to natural fires and accordingly the total concentration of charcoal was low during this interval (Fried et al., 2004). The grain-size distribution curves are unimodal and the cumulative curve indicates a single stage and hence a single mode of sediment transport. The absence of creep and saltation components indicates that hydrodynamic forces were weak, which may indicate a lacustrine sedimentary environment. The immediate environment of the site—a large lake with a high water level—unfavorable living space for hominins. During the interval of 1.333–1.324 Ma the pollen assemblage changed from tree-dominated to herb-dominated, mainly *Artemisia*, Chenopodiaceae, Poaceae and *Urtica + Hunulus*. Indicating that the environment had changed from the previous forest to a steppe landscape. The sample scores on PCA axis 1 (**Figure 7**) are negative and those on axis 2 are positive, indicating that the climate was cold and dry. The pollen concentration (6 grains/g) and charcoal concentration (300 particles/g) were also the lowest during the studied interval, which is compatible with a cold and arid climate. The grain-size distribution curves are bimodal and the cumulative curve has two stages; the suspended sediment component was largely replaced by a saltation component (with a representation >50%), indicating an increased fluvial influence on sedimentation. The change in the sedimentary environment may have been related to the contraction of the lake under a substantially drier climate than during the previous stage. The site would have been located some distance from the lake and the sediments were largely delivered by runoff, represented by lower pollen concentrations at this stage.

## Environmental Characteristics of the Banshan Site During the Interval of Hominin Occupation (1.324–1.317 Ma)

The interval of hominin activity at the Banshan site was mainly during 1.324–1.317 Ma. The pollen assemblage during this interval was dominated by *Pinus*, and the herb pollen representation was ~ 30%, indicating that the regional vegetation was mainly forest, but with substantial numbers of herbaceous plants. In addition, there are some animal fossils which adapted to a forest environment in the artefact layer of the site, included *Elephantids*, *Cervids* and *Rhinocerotids*; while, there are also some animal fossils, adapted grassland environment, e.g., *Equus*; also some amphiphilic animals such as *Canis* (Wei, 1994). These findings also indicate that in addition to forest, there were also areas of grassland. Sample scores on PCA axis 1 are positive, indicating a wet climate and that hominin activity in the area was initiated during the period when the climate changed from cold to warm and wet, which is roughly equivalent to marine isotope stage (MIS) 41 (Lisiecki and Raymo, 2005; Channell et al., 2016). The stage began with a change from weak to strong Northern Hemisphere insolation (Berger and Loutre, 1991) and summer monsoon index from Nihewan Basin (Ao et al., 2012b) with resulting rapid climatic warming. In addition, the results are roughly consistent with the variation trend of temperature reconstruction (MAT) on the eastern Tibetan Plateau (Zhao et al., 2021) (**Figure 7**). In the Chinese loess-paleosol stratigraphy, this period is roughly equivalent to S16, characterized by minor magnetic susceptibility variations, indicating a warm relatively stable climate (Ding et al., 2002; Sun et al., 2006; Sun et al., 2010). During the same interval in Iberia, hominin sites in the Guadix-Baza Basin (dated to 1.4–1.3 Ma) also show that ancient humans occupied a forested lake margin environment, under a warm and wet climate (Altolaguirre et al., 2021).

The grain-size cumulative curve shows that the sediments during this interval were dominated by a saltation component (with a content of 70%, which is slightly higher than during the previous interval), with a suspended component of 25% and a minor suspended component. These characteristics suggest a stable high-energy hydrodynamic environment (Zhang et al., 2018). The grain-size frequency distribution curves of a few samples are bimodal, but most of the curves are unimodal, with the mode concentrated below 35 μm, which is characteristic of transport in suspension (Middleton, 1976). The pollen data indicate a change to a warm and humid climate, and the increased precipitation may have led to increased surface runoff; hence, the grain size became coarser and the suspended component increased (Sun et al., 2001). The site was likely a floodplain or lakeside environment.

The charcoal particles show the highest concentration during hominin occupation period than that in other periods, with 8.2 times higher than that before the appearance of hominins and 6.5 times higher than that after the end of hominin activity. More over, the charcoal content of medium and coarse particles is also much higher than that in the other two periods, indicating that local fires occurred more frequently (Miao et al., 2016; Shi et al., 2020). One hand, the high frequency local fires may be related to artificial fire. The earliest evidence of artificial fire in China can be traced back to Yuanmou (1.8 Ma) sites (Jia and Wang, 1978), which is older than Banshan site. but direct archaeological evidence of artificial fire in Bashan site is still absent. On the other hand, it maybe come from wildfire. Even it was the wildfire, which still benefit for the huminid survive. Studies on the behavior of modern primates in Africa have shown that some primates can not only coexist peacefully with wildfire, but forage in the fire-modified landscape (Herzog et al., 2016; Pruetz and Herzog, 2017). This might also be the case of huminid facing wildfire (Gao, 2020). It can be seen that himinins at Banshan site can benefited from whether artificial fire or wildfire.

## Environmental Characteristics After the End of Hominin Activity

After the termination of paleo-human activity at the Banshan site (1.317–1.290 Ma), the climate continued to be warm and wet but a drying trend then commenced and the forest vegetation gradually declined. The pollen record indicates that the environment during this interval can be divided into two stages. During the first stage (1.317–1.312 Ma), the pollen assemblages are consistent with the animal fossil assemblages of the cultural layer, indicating that the warm and humid climate lasted until ~ 1.312 Ma. The termination of local hominin activity may have related to the rise in the lake level. The grain size cumulative curve shows a single stage, consistent with a lacustrine deposit which may led to the decrease of charcoal concentration. It is possible that the continuous warm and wet climate caused the shoreline of the Nihewan ancient lake to expand landward and the site was submerged. This scenario is consistent with the understanding of the Turkana Basin in Africa (Roach et al., 2018). The influence of lake expansion and contraction on paleo-human activities was mainly manifested by the consistency of the location of hominin activity with the shifts in the lakeside zone. Therefore, we conclude that the expansion of the lake was a least one of the reasons for the disappearance of hominin activity at the site.

During the second stage (1.312–1.290 Ma), the pollen assemblage was dominated by herbs, especially *Artemisia*. Drought-tolerant shrubs (e.g., Elaeagnaceae) increased, and most of the tree pollen content less than 30%, indicating that the vegetation had degenerated to steppe or forest steppe. Sample scores on PCA axis 1 and axis 2 are negative, indicating that the climate was becoming dry. The charcoal concentration decreased substantially, suggesting a decrease in the biomass due to climatic drying. The grain size cumulative curve shows three well defined stages, with a saltation component of nearly 70%, and the appearance of a creep component, indicating a strengthened fluvial influence and suggesting that the lake had contracted which resulted in the deposition of fluvial facies. Compared with the previous stage, the climate became dry which would not have provided a habitat favorable for ancient humans. Shrinking lakes and the decreasing biomass would likely have caused a reduction in available food and water resources for humans.

## CONCLUSION

1) Before the appearance of hominin activity at the Banshan site (1.337–1.324 Ma), the climate of the region was generally cold, with fluctuations between cold-wet and cold-dry conditions.

The vegetation changed from forest dominated by *Pinus* and *Picea* to grassland dominated by plants tolerant of dry conditions, such as *Artemisia* and Chenopodiaceae.

2) During the period of hominin activity (1.324–1.317 Ma), the climate was warm and wet and the vegetation was mainly *Pinus* forest; however, the forest cover was not high since herbaceous plants are well represented in the pollen record. The site was located on the lake margin.

3) A warm and humid climate during 1.317–1.312 Ma led to the continuous expansion of the lake and the lake level rose. The site was a lacustrine environment and hominins were likely forced to migrate outside the area. During 1.312–1.290 Ma the climate changed from warm and wet to cold and dry, and the vegetation changed from forest to grassland again (Xu et al., 2017).

## DATA AVAILABILITY STATEMENT

The original contributions presented in the study are included in the article/Supplementary Material, further inquiries can be directed to the corresponding authors.

## REFERENCES

Altolaguirre, Y., Schulz, M., Gibert, L., and Bruch, A. A. (2021). Mapping Early Pleistocene Environments and the Availability of Plant Food as a Potential Driver of Early Homo Presence in the Guadix-Baza Basin (Spain). *J. Hum. Evol.* 155, 102986. doi:10.1016/j.jhevol.2021.102986

Ao, H., An, Z., Dekkers, M. J., Wei, Q., Pei, S., Zhao, H., et al. (2012a). High-resolution Record of Geomagnetic Excursions in the Matuyama Chron Constrains the Ages of the Feiliang and Lanpo Paleolithic Sites in the Nihewan Basin, North China. *Geochem. Geophys. Geosyst.* 13, a–n. doi:10.1029/2012GC004095

Ao, H., Dekkers, M. J., Xiao, G., Yang, X., Qin, L., Liu, X., et al. (2012b). Different Orbital Rhythms in the Asian Summer Monsoon Records from North and South China during the Pleistocene. *Glob. Planet. Change* 80-81, 51–60. doi:10.1016/j.gloplacha.2011.09.012

Ao, H., Dekkers, M. J., Wei, Q., Qiang, X., and Xiao, G. (2013a). New Evidence for Early Presence of Hominids in North China. *Sci. Rep.* 3, 2403. doi:10.1038/srep02403

Ao, H., An, Z., Dekkers, M. J., Li, Y., Xiao, G., Zhao, H., et al. (2013b). Pleistocene Magnetochronology of the Fauna and Paleolithic Sites in the Nihewan Basin: Significance for Environmental and Hominin Evolution in North China. *Quat. Geochronol.* 18, 78–92. doi:10.1016/j.quageo.2013.06.004

Ao, H., Dekkers, M. J., An, Z., Xiao, G., Li, Y., Zhao, H., et al. (2013c). Magnetostratigraphic Evidence of a Mid-pliocene Onset of the Nihewan Formation - Implications for Early Fauna and Hominid Occupation in the Nihewan Basin, North China. *Quat. Sci. Rev.* 59, 30–42. doi:10.1016/j.quascirev.2012.10.025

Ao, H., Liu, C.-R., Roberts, A. P., Zhang, P., and Xu, X. (2017). An Updated Age for the Xujiayao Hominin from the Nihewan Basin, North China: Implications for Middle Pleistocene Human Evolution in East Asia. *J. Hum. Evol.* 106, 54–65. doi:10.1016/j.jhevol.2017.01.014

Bailey, I., Foster, G. L., Wilson, P. A., Jovane, L., Storey, C. D., Trueman, C. N., et al. (2012). Flux and Provenance of Ice-Rafted Debris in the Earliest Pleistocene Sub-polar North Atlantic Ocean Comparable to the Last Glacial Maximum. *Earth Planet. Sci. Lett.* 341-344, 222–233. doi:10.1016/j.epsl.2012.05.034

Barbour, G. B. (1924). Preliminary Observation in Kalgan Area. *Bull. Geol. Surv. Can.* 3, 167–168.

Berger, A., and Loutre, M. F. (1991). Insolation Values for the Climate of the Last 10 Million Years. *Quat. Sci. Rev.* 10, 297–317. doi:10.1016/0277-3791(91)90033-Q

## AUTHOR CONTRIBUTIONS

JY: Conceptualization, Writing–Original Draft and Review, Visualization, Software, Formal analysis ZZ: Conceptualization, Writing–Original Draft and Review YL: Conceptualization, Writing–Review and Editing, Funding acquisition FW: Methodology, Validation and Formal analysis BF: Software, Validation and Formal analysis HX: Software, Formal analysis ZS: Software, Formal analysis SW: Formal analysis SD: Formal analysis.

## FUNDING

## ACKNOWLEDGMENTS

Bonnefille, R. (2010). Cenozoic Vegetation, Climate Changes and Hominid Evolution in Tropical Africa. *Glob. Planet. Change* 72, 390–411. doi:10.1016/j.gloplacha.2010.01.015

Braak, T., and Smilauer, P. N. (2012). *Canoco Reference Manual and User's Guide: Software for Ordination, Version 5.0.* Ithaca USA: Microcomputer Power, 496.

Channell, J. E. T., Hodell, D. A., and Curtis, J. H. (2016). Relative Paleointensity (RPI) and Oxygen Isotope Stratigraphy at IODP Site U1308: North Atlantic RPI Stack for 1.2-2.2 Ma (NARPI-2200) and Age of the Olduvai Subchron. *Quat. Sci. Rev.* 131, 1–19. doi:10.1016/j.quascirev.2015.10.011

Chen, C., Shen, C., Chen, W. Y., and Tang, Y. J. (1999). 1998 Excavation of the Xiaochangliang Site at YangYuan, HeBei. *Acta Anthropol. Sin.* 18, 225–239. (in Chinese with English abstract). doi:10.16359/j.cnki.cn11-1963/q.1999.03.006

Chen, M. N. (1988). *Study on the Nihewan Formation.* Beijing: Maritime Press, 1–145. (in Chinese).

Colcord, D. E., Shilling, A. M., Sauer, P. E., Freeman, K. H., Njau, J. K., Stanistreet, I. G., et al. (2018). Sub-Milankovitch Paleoclimatic and Paleoenvironmental Variability in East Africa Recorded by Pleistocene Lacustrine Sediments from Olduvai Gorge, Tanzania. *Palaeogeogr. Palaeoclimatol. Palaeoecol.* 495, 284–291. doi:10.1016/j.palaeo.2018.01.023

Davies, C. P., and Fall, P. L. (2001). Modern Pollen Precipitation from an Elevational Transect in central Jordan and its Relationship to Vegetation. *J. Biogeogr.* 28, 1195–1210. doi:10.1046/j.1365-2699.2001.00630.x

Deng, C., Wei, Q., Zhu, R., Wang, H., Zhang, R., Ao, h., et al. (2006). Magnetostratigraphic Age of the Xiantai Paleolithic Site in the Nihewan Basin and Implications for Early Human Colonization of Northeast Asia. *Earth Planet. Sci. Lett.* 244, 336–348. doi:10.1016/j.epsl.2006.02.001

Deng, C., Zhu, R., Zhang, R., Ao, H., and Pan, Y. (2008). Timing of the Nihewan Formation and Faunas. *Quat. Res.* 69, 77–90. doi:10.1016/j.yqres.2007.10.006

Deng, C., Hao, Q., Guo, Z., and Zhu, R. (2019). Quaternary Integrative Stratigraphy and Timescale of China. *Sci. China Earth Sci.* 62, 324–348. doi:10.1007/s11430-017-9195-4

Dennell, R. W. (2013). The Nihewan Basin of North China in the Early Pleistocene: Continuous and Flourishing, or Discontinuous, Infrequent and Ephemeral Occupation. *Quat. Int.* 295, 223–236. doi:10.1016/j.quaint.2012.02.012

Ding, Z. L., Derbyshire, E., Yang, S. L., Yu, Z. W., Xiong, S. F., and Liu, T. S. (2002). Stacked 2.6-Ma Grain Size Record from the Chinese Loess Based on Five Sections and Correlation with the Deep-Sea δ18O Record. *Paleoceanography* 17, 5–1. doi:10.1029/2001PA000725

Ding, G., Li, Y., Zhang, Z., Zhang, W., Wang, Y., Chi, Z., et al. (2020). Vegetation Succession and Climate Change during the Early Pleistocene (2.2-1.8 Ma) in the

Nihewan Basin, Northern China. *Palaeogeogr. Palaeoclimatol. Palaeoecol.* 537, 109375. doi:10.1016/j.palaeo.2019.109375

Faegri, K., and Iversen, J. (1989). *Textbook of Pollen Analysis*. fourth ed. Chichester, UK: Wiley.

Fried, J. S., Torn, M. S., and Mills, E. (2004). The Impact of Climate Change on Wildfire Severity: A Regional Forecast for Northern California. *Climatic Change* 64, 169–191. doi:10.1023/b:clim.0000024667.89579.ed

Friedman, G. M., and Sanders, J. E. (1978). *Principles of Sedimentology*. New Jersey: Wiley.

Gao, X. (2020). Fire for Hominin Survivals in Prehistory. *Acta Anthropol. Sin.* 39, 333–348. (in Chinese with English abstract). doi:10.16359/j.cnki.cn11-1963/q. 2020.0008

Guan, Y., Wang, F.-G., Xie, F., Pei, S.-W., Zhou, Z.-Y., and Gao, X. (2016). Flint Knapping Strategies at Cenjiawan, an Early Paleolithic Site in the Nihewan Basin, North China. *Quat. Int.* 400, 86–92. doi:10.1016/j.quaint.2015.07.008

Herzog, N. M., Keefe, E. R., Parker, C. H., and Hawkes, K. (2016). What's Burning Got to Do with it? Primate Foraging Opportunities in Fire-Modified Landscapes. *Am. J. Phys. Anthropol.* 159, 432–441. doi:10.1002/ajpa.22885

Hou, Y. M. (2003). Naming and Preliminary Study on the Category of the "Donggutuo Core". *Acta Anthropol. Sin.* 22, 279–292. (in Chinese with English abstract). doi:10.1023/a:1023407424369

Jia, L. P., and Wang, J. (1978). *Xihoudu: Early Pleistocene Ancient Cultural Sites in Shanxi*. Beijing: Cultural Relics Press. (in Chinese).

Jiang, Z. X. (2010). *Sedimentology*. Beijng: Petroleum Industry Press, 50–55. (in Chinese).

Leinen, M., and Heath, G. R. (1981). Sedimentary Indicators of Atmospheric Activity in the Northern Hemisphere during the Cenozoic. *Palaeogeogr. Palaeoclimatol. Palaeoecol.* 36, 1–21. doi:10.1016/0031-0182(81)90046-8

Li, Y. C., Xu, Q. H., and Yang, X. L. (1996). Pollen Analysis of Feiliang Site in Yangyuan , Hebei. *Geo. Territor. Res.* 12, 56–60. (in Chinese).

Li, Y. C., Ding, G. Q., Wang, Y., Chi, Z. Q., Yang, X. L., and Li, B. (2018). Early Pleistocene (2.6-2.1Ma) Vegetation and Climate Changes in the Nihewan Basin. *Quat. Sci.* 38 (4), 830–841. doi:10.11928/j.issn.1001-7410.2018.04.03

Li, Y., Zhang, Z., Ding, G., Xu, Q., Wang, Y., Chi, Z., et al. (2019). Late Pliocene and Early Pleistocene Vegetation and Climate Change Revealed by a Pollen Record from Nihewan Basin, North China. *Quat. Sci. Rev.* 222, 105905. doi:10.1016/j. quascirev.2019.105905

Lisiecki, L. E., and Raymo, M. E. (2005). A Pliocene-Pleistocene Stack of 57 Globally Distributed Benthic δ18O Records. *Paleoceanography* 20, a–n. doi:10. 1029/2004PA001071

Liu, Y., Hu, Y., and Wei, Q. (2013). Early to Late Pleistocene Human Settlements and the Evolution of Lithic Technology in the Nihewan Basin, North China: A Macroscopic Perspective. *Quat. Int.* 295, 204–214. doi:10.1016/j.quaint.2012. 01.015

Liu, P., Yue, F., Liu, J., Qin, H., Li, S., Zhao, X., et al. (2018). Magnetostratigraphic Dating of the Shixia Red Sediments and Implications for Formation of Nihewan paleo-lake, North China. *Quat. Sci. Rev.* 193, 118–128. doi:10.1016/j.quascirev. 2018.06.013

Lu, H., Wu, N., Liu, K.-b., Zhu, L., Yang, X., Yao, T., et al. (2011). Modern Pollen Distributions in Qinghai-Tibetan Plateau and the Development of Transfer Functions for Reconstructing Holocene Environmental Changes. *Quat. Sci. Rev.* 30, 947–966. doi:10.1016/j.quascirev.2011.01.008

Miao, Y., Fang, X., Song, C., Yan, X., Zhang, P., Meng, Q., et al. (2016). Late Cenozoic Fire Enhancement Response to Aridification in Mid-latitude Asia: Evidence from Microcharcoal Records. *Quat. Sci. Rev.* 139, 53–66. doi:10.1016/ j.quascirev.2016.02.030

Middleton, G. V. (1976). Hydraulic Interpretation of Sand Size Distributions. *J. Geology.* 84 (4), 405–426. doi:10.1086/628208

Pei, S. W. (2002). The Paleolithic Site at Dachangliang in Nihewan Basin, North China. *Acta Anthropol. Sin.* 21, 116–125. (in Chinese with English abstract). doi:10.16359/j.cnki.cn11-1963/q.2002.02.004

Pei, S., Li, X., Liu, D., Ma, N., and Peng, F. (2009). Preliminary Study on the Living Environment of Hominids at the Donggutuo Site, Nihewan Basin. *Chin. Sci. Bull.* 54, 3896–3904. doi:10.1007/s11434-009-0646-9

Pei, S., Xie, F., Deng, C., Jia, Z., Wang, X., Guan, Y., et al. (2017). Early Pleistocene Archaeological Occurrences at the Feiliang Site, and the Archaeology of Human Origins in the Nihewan Basin, North China. *Plos. ONE* 12, e0187251. doi:10. 1371/journal.pone.0187251

Peng, Y., Xiao, J., Nakamura, T., Liu, B., and Inouchi, Y. (2005). Holocene East Asian Monsoonal Precipitation Pattern Revealed by Grain-Size Distribution of Core Sediments of Daihai Lake in Inner Mongolia of north-central China. *Earth Planet. Sci. Lett.* 233, 467–479. doi:10.1016/j.epsl.2005.02.022

Pruetz, D. S., and Herzog, M. N. (2017). Savanna Chimpanzees at Fongoli, Senegal, Navigate a Fire Landscape. *Curr. Anthropol.* 58, 337–350. doi:10.1086/692112

Roach, N. T., Du, A., Hatala, K. G., Ostrofsky, K. R., Reeves, J. S., Braun, D. R., et al. (2018). Pleistocene Animal Communities of a 1.5 Million-Year-Old Lake Margin Grassland and Their Relationship to Homo Erectus Paleoecology. *J. Hum. Evol.* 122, 70–83. doi:10.1016/j.jhevol.2018.04.014

Shi, Y., Pan, B., Wei, M., Li, X., Cai, M., Wang, J., et al. (2020). Wildfire Evolution and Response to Climate Change in the Yinchuan Basin during the Past 1.5 Ma Based on the Charcoal Records of the PL02 Core. *Quat. Sci. Rev.* 241, 106393. doi:10.1016/j.quascirev.2020.106393

Sun, X. J., Wang, F. Y., and Song, C. Q. (1996). Pollen of Some Families and Genera in Northern China—Climate Response Surface Analysis. *Sci. China D* 26, 431–436. doi:10.1360/yd1996-39-5-486

Sun, D. H., An, Z. S., Su, R. X., Wu, X. H., Wang, S. M., Sun, Q. L., et al. (2001). A Mathematical Method for the Separation of Grain Size Components from Sediments in Paleoenvironment and its Application. *Prog. Nat. Sci.* 11, 47–54. (in Chinese). doi:10.3321/j.issn:1002-008X.2001.03.008

Sun, Y., Clemens, S. C., An, Z., and Yu, Z. (2006). Astronomical Timescale and Palaeoclimatic Implication of Stacked 3.6-Myr Monsoon Records from the Chinese Loess Plateau. *Quat. Sci. Rev.* 25, 33–48. doi:10.1016/j.quascirev.2005. 07.005

Sun, Y., An, Z., Clemens, S. C., Bloemendal, J., and Vandenberghe, J. (2010). Seven Million Years of Wind and Precipitation Variability on the Chinese Loess Plateau. *Earth Planet. Sci. Lett.* 297, 525–535. doi:10.1016/j.epsl.2010.07.004

Tang, Y. J., Li, Y., and Chen, W. Y. (1995). Mammalian Fossols and the Age of Xiaochangliang Paleolithic Site of YangYuan. *Hebei. Vertebrata. Palasiatica.* 33, 225–239. (in Chinese with English abstract). doi:10.19615/j.cnki.1000-3118. 1995.01.013

Tang, L. Y., Mao, L. M., Shu, J. W., Li, C. H., Shen, C. M., and Zhou, Z. Z. (2016). *An Illustrated Handbook of Quaternary Pollen and Spores in China*. Beijing: Science Press. (in Chinese).

Wang, F. X., Qian, N. F., Zhang, Y. L., and Yang, H. Q. (1995). *Pollen Flora of China*. second ed. Beijing: Science Press. (in Chinese).

Wang, X., Yang, Z., Løvlie, R., and Min, L. (2004). High-resolution Magnetic Stratigraphy of Fluvio-Lacustrine Succession in the Nihewan Basin, China. *Quat. Sci. Rev.* 23, 1187–1198. doi:10.1016/j.quascirev.2003.11.007

Wang, H., Deng, C., Zhu, R., and Xie, F. (2006). Paleomagnetic Dating of the Cenjiawan Paleolithic Site in the Nihewan Basin, Northern China. *Sci. China Ser. D* 49, 295–303. doi:10.1007/s11430-006-0295-7

Wei, Q. (1994). Banshan Paleolithic Site from the Lower Pleistocene in the Nihewan Basin in North China. *Acta Anthropol. Sin.* 13, 223–238. (in Chinese with English abstract). doi:10.16359/j.cnki.cn11-1963/q.1994.03.003

Wei, Q. (2014). New Observations on Stone Artifacts from the Donggutuo Site. *Acta Anthropol. Sin.* 33, 254–269. (in Chinese with English abstract). doi:10. 16359/j.cnki.cn11-1963/q.2014.03.007

Xia, Z. K., and Liu, X. Q. (1984). On Paleography of the Nihewan Basin during the Accumulation of Nihewan Serise. *Mar. Geol. Quat. Geol.* 4, 101–110. (in Chinese with English abstract). doi:10.16562/j.cnki.0256-1492.1984.03.011

Xie, F., and Cheng, S. (1990). Paleoliths Excavated in Cenjiawan Village, YangYuan, HeBei Province. *Acta Anthropol. Sin.* 9, 265–272. (in Chinese with English abstract). doi:10.16359/j.cnki.cn11-1963/q.1990.03.013

Xie, F., Li, J., and Liu, L. Q. (2004). *Nihewan Paleolithic Culture*. Shijiazhuang: Huashan literature and Art Press, 80–107. (in Chinese).

Xie, F. (2006). *Nihewan*. Beijing: Cultural Relics Press, 13–224. (in Chinese).

Xu, Y. Z., Li, Y. Y., Liu, G. X., and Zhou, L. P. (2017). Quantitative Reconstruction of Past Vegetation Around Gangga Archaeological Site in Hulunbuir Steppe, China. *Quat. Sci.* 37, 1391–1402. doi:10.11928/j.issn.1001-7410.2017.06.21

Yang, S.-X., Hou, Y.-M., Yue, J.-P., Petraglia, M. D., Deng, C.-L., and Zhu, R.-X. (2016). The Lithic Assemblages of Xiaochangliang, Nihewan Basin: Implications for Early Pleistocene Hominin Behaviour in North China. *PLoS .ONE* 11, e0155793. doi:10.1371/journal.pone.0155793

Yang, S. X., Deng, C. L., Zhu, R. X., and Petraglia, M. D. (2020). The Paleolithic in the Nihewan Basin, China: Evolutionary History of an Early to Late Pleistocene Record in Eastern Asia. *Evol. Anthropol.* 29, 125–142. doi:10.1002/evan.21813

Yuan, B. Y., Xia, Z. K., and Niu, P. S. (2011). *Nihewan Rift and Early Man*. Beijing: Geology Press, 12–20. (in Chinese).

Yuan, J., Wang, G. M., Xu, F. J., and Yan, J. H. (2013). *Principles of Sedimentology*. Beijng: Geological Press, 135–156. (in Chinese).

Zhang, W. C., Li, C. H., Lu, H. Y., Tian, X. H., Zhang, H. Y., Lei, F., et al. (2013). Relationship between Surface Pollen Assemblage and the Vegetation in Luonan Basin, Eastern Qinling Mountains, Central China. *Acta Geophys. Sin.* 68, 398–413. (in Chinese with English abstract). doi:10.1007/s11442-014-1098-y

Zhang, J. R., Yang, H. F., Han, J. B., Li, Q., and Liu, W. C. (2018). Application of Probability Cumulative Grain Size Curves and Lithofacies Association to Sedimentology. *Nat. Gas. Tech. Econ.* 12, 20–23. (in Chinese with English abstract). doi:10.3969/j.issn.2095-1132.2018.04.006

Zhang, Z., Li, Y., Li, C., Xu, Q., Zhang, R., Ge, Y., et al. (2020). Pollen Evidence for the Environmental Context of the Early Pleistocene Xiashagou Fauna of the Nihewan Basin, north China. *Quat. Sci. Rev.* 236, 106298. doi:10.1016/j.quascirev.2020.106298

Zhang, Z., Li, Y., Ding, G., Fan, B., Da, S., Xu, Q., et al. (2022). Astronomical Forcing of Vegetation and Climate Change during the Late Pliocene-Early Pleistocene of the Nihewan Basin, North China. *Quat. Int.* 613, 1–13. doi:10.1016/j.quaint.2021.07.017

Zhao, Y., Xu, Q., Huang, X., Guo, X., and Tao, S. (2009). Differences of Modern Pollen Assemblages from lake Sediments and Surface Soils in Arid and Semi-arid China and Their Significance for Pollen-Based Quantitative Climate Reconstruction. *Rev. Palaeobotany Palynology* 156, 519–524. doi:10.1016/j.revpalbo.2009.05.001

Zhao, Y., Liang, C., Cui, Q., Qin, F., Zheng, Z., Xiao, X., et al. (2021). Temperature Reconstructions for the Last 1.74-Ma on the Eastern Tibetan Plateau Based on a Novel Pollen-Based Quantitative Method. *Glob. Planet. Change* 199, 103433. doi:10.1016/j.gloplacha.2021.103433

Zhou, T. R., Li, H. Z., Liu, Q. S., Li, R. Q., and Sun, X. P. (1991). *Cenozoic Paleography Research of Nihewan basin*. Beijing: Science Press, 1–46. (in Chinese).

Zhu, R. X., Hoffman, K. A., Potts, R., Deng, C. L., Pan, Y. X., Guo, B., et al. (2001). Earliest Presence of Humans in Northeast Asia. *Nature* 413, 413–417. doi:10.1038/35096551

Zhu, R. X., Potts, R., Xie, F., Hoffman, K. A., Deng, C. L., Shi, C. D., et al. (2004). New Evidence on the Earliest Human Presence at High Northern Latitudes in Northeast Asia. *Nature* 431, 559–562. doi:10.1038/nature02829

Zuo, T., Cheng, H., Liu, P., Xie, F., and Deng, C. (2011). Magnetostratigraphic Dating of the Hougou Paleolithic Site in the Nihewan Basin, North China. *Sci. China Earth Sci.* 54, 1643–1650. doi:10.1007/s11430-011-4221-2